Examining Copper-dependent Cell Death-associated Genes in Relation to Immune Cell Presence and Disease Outcomes in Stomach Adenocarcinoma

Jinyuan Li, Huixia Rao, Huanhuan Guo, Wenhong Liao, Sijia Xia, Xinyue Wang, Rongbin Pan*, Yongcui Liao*, Dacheng Zhu*

Jiangxi University of Chinese Medicine, Nanchang 330004, Jiangxi, China

*Corresponding author

Abstract: Cuproptosis represents a novel class of cell death modality different from other regulated cell death pathways. However, the role of genes involved in copper-mediated cell death within the tumor microenvironment of gastric adenocarcinoma remains to be elucidated. This study utilized R programming to classify unprocessed information from TCGA and GEO repositories of individuals with stomach adenocarcinoma. Associations among various patient clusters, clinical factors, immune cell infiltration attributes, and the tumor microenvironment were assessed. Graphical displays were generated to improve the practical utility of copper-dependent cell death gene scores and evaluate patient outcome probabilities. This work sought to examine the links between copper-mediated cell death and molecular traits, immune cell presence in the tumor, patient outcomes, and therapeutic approaches. A copper-dependent cell death gene score was developed to predict patient survival and assess its prognostic value in stomach adenocarcinoma. Results revealed that reduced copper-mediated cell death scores correlated with increased tumor mutations, immune responsiveness, and greater survival rates, while elevated scores were linked to suppressed immunity and enhanced tumor microenvironment signaling. This study additionally determined prognostic factors related to copper-dependent cell death genes in stomach adenocarcinoma, which could elucidate qualities of the tumor surroundings and aid in the development of enhanced immunotherapeutic approaches.

***Keywords*:** cuproptosis; biomarkers; stomach adenocarcinoma; immunotherapy

1. Introduction

Gastric adenocarcinoma arises from the epithelial lining of the stomach, with adenocarcinomas comprising over 90% of stomach cancer diagnoses [1]. The annual global incidence exceeds 990,000 cases, resulting in approximately 738,000 deaths [2]. The second deadliest cancer globally and the fourth most prevalent form to be diagnosed is gastric cancer. [3]. Stomach cancer imparts substantial strain on medical systems globally [4]. Long-term survival rates remain poor, with 5-year survival around 20% [5]. Although endoscopy is essential for diagnosing gastric malignancies, its cost and invasiveness pose significant barriers for many individuals [6], highlighting the need for non-invasive diagnostic markers [7]. Up to now, STAD treatment mainly relies on radiation and surgery, as there are no specific drugs available.. However, these methods have failed to significantly improve patient survival, making the identification of efficacious treatment targets and prognostic indicators crucial for extending survival in gastric adenocarcinoma.

Cancer immunotherapy aims to activate anti-tumor immunity, manage and eradicate tumors, using targeted antibodies, inhibitors and other therapies. Immunological checkpoints, including CTLA-4 and PD-1, are membrane-bound particles predominantly present on T lymphocytes. When the checkpoint binds to the ligand, it inhibits the initiation and intensity of the immune response [8-9]. Checkpoint inhibitors re-establish the anti-cancer function of killer T cells through impeding these immunological checkpoints or their binding partners. The effectiveness of ICIs has been confirmed by numerous clinical studies. For example, immunotherapeutic approaches have the potential to elevate the 3-year survival rate in SCLC patients to 31%, a nearly threefold improvement compared to chemotherapy alone [10-11]. However, some patients with SCLC have shown resistance to this treatment [12]. Although ICIs have been effective in some cancer clinical trials, such as metastatic melanoma, their effectiveness in treating most solid cancers is still limited. [13-15]. These findings suggest that depending solely on current biomarkers is insufficient for precisely evaluating patient outcomes and choosing optimal treatment approaches. As a result, an urgent requirement exists for discovering innovative biomarkers and predictive frameworks capable of addressing the evident diversity in disease outcomes.

Copper is an essential trace element for living organisms, and its concentration balance is crucial for maintaining the normal functioning of biological systems. Copper deficiency can inhibit enzyme activity, while excess can trigger cell death [16]. Excessive copper can trigger a novel cell death mechanism - mitochondrial dependent copper mutations, which bind

to lipid modified citric acid cycling components, leading to protein aggregation, iron sulfur cluster depletion, and stress response, ultimately triggering cell death. In addition, copper serves as a key cofactor for various enzymes, participating in numerous enzyme pathways and important biological functions. Although the levels of copper ions within the body are maintained in a fluid balance, perturbations to this balance result in cellular toxicity and the activation of cellular death via diverse mechanisms. Recent studies have shown that copper poisoning is closely related to cancer development, prognosis, and treatment, and can induce cell anti-tumor activity and inhibit STAD cell growth. Moreover, copper is associated with the formation, proliferation, and dissemination of cancerous growths. Nevertheless, STAD cells lack several cuproptosis-related genes [17,18,19,20,21].

Our research utilized computational techniques to examine information from cancer genomics repositories to explore how genes associated with this novel cell death pathway impact cancer advancement, the cellular milieu within tumors, response to immunotherapy, and patient outcomes in stomach cancer. Moreover, stomach cancer patients were categorized into separate cohorts to assess differences in diagnostic value, genetic features, treatment response, and immune cell presence. Have developed a prognostic model for cell death gene expression to accurately predict cancer prognosis, aiming to elucidate the relationship between new cell death pathways and gastric malignant tumors, and explore new immunotherapy methods.

2. Materials and Methods

2.1 Data sources

Download the GSE84433 dataset from the Public Genomics Library, which contains microarray gene expression data from 413 patients, for analysis.

Genes involved in the cell death pathway were identified through a review of published studies, and information was collected from genomic and gene annotation databases. Additional analyses utilized RNA sequencing information from the same microarray and a cohort of stomach adenocarcinoma patients. Genetic alteration information was acquired from the same cancer genomic repositories. The RNA quantification analyzed in this research originated from the aforementioned databases after acquiring the unprocessed data and performing quality control and standardization. A statistical technique was applied to correct for technical variation unrelated to the biological conditions[22,23].

2.2 Data processing and differential screening

Genes with significantly different expression levels in the microarray were determined using a linear modeling approach in the R programming language. Genes were considered differentially expressed if they met a minimum fold-change magnitude and statistical significance threshold. Visual representations of the gene expression patterns were created using R graphing libraries.

2.3 GO and KEGG enrichment analysis

This study used the clusterProfiler R package for GO, KEGG, and other analyses to elucidate the biological roles, processes, and genomic enrichment of differentially expressed genes [24-25]

2.4 CRG genotyping

We assessed genes in the combined TCGA and GEO data for survival associations via Cox regression to determine prognostic categories. Genes with $p<0.05$ based on cuproptosis-related gene expression across samples were filtered out, and samples were categorized into A and B groups using the Cluster R package. A gene cluster was generated using the CRGs-based prognosis-related genes, and the tumor pattern was quantified using the "NMF" software. Patients are divided into high and low risk groups, and their clinical characteristics and survival outcomes are compared.

2.5 Relationship between molecular patterns, clinical characteristics and TME

Kaplan Meier analysis evaluated the impact of the evaluation mode on survival rate, and STAD patients also calculated matrix and immune scores.Examined how the two subgroups connected with the main immunological checkpoint gene expression.The Immunocore R function quantifies immune infiltration in high-risk and low-risk groups, evaluates the number of immune cells through classification [26-27], compares the proportion of immune cells in the tumor microenvironment, and studies the functions and relationships of 22 immune cells in copper toxicity related genomes. Within each category, changes in immune checkpoint expression were evaluated using Spearman analysis.

2.6 Survival analysis of cuproptosis subtypes

Kaplan Meier analysis was used to evaluate the survival rate of high-risk groups, and PCA, t-SNE, and dimensional analysis were used to show differences. Cox analysis confirmed that copper toxicity gene scores independently predicted

prognosis. The concordance index, calibration curves, and decision curve analysis evaluated the predictive power of the column plots. ROC curves that varied with time were generated at 1, 3, and 5 years with the timeROC R package [28] to validate the predictive performance of the created column charts.

2.7 Examination of the tumor's microsatellite instability and mutation burden

Use maftools to analyze gene mutations in risk groups and explore the relationship between CRG scores and TMB. Use Survminer to find the optimal cutting point score for TMB patients in the low high TMB group, and comprehensively analyze the effects of TMB and CRG scores on OS, as well as the relationship between CRG score and MSI.

2.8 Drug sensitivity analysis

Calculated the IC50 values of drugs to assess treatment efficacy, compared drug sensitivity between high-risk and low-risk groups, and searched for relevant drugs in the GDSC database. At the same time, the immune phenotype scores of each subgroup of STAD patients were evaluated, and the research results were obtained from the Cancer Imaging Archive.

2.9 Statistical analysis

Log-rank tests and R survival package analysis were employed to evaluate the survival rates for different groups. Furthermore, Wilcoxon tests were applied for pairwise data group comparisons, while Kruskal-Wallis tests were utilized when comparing three or more data groups [29]. Survival curves for each subgroup were generated using Kaplan-Meier analysis. Chi-square tests were performed to evaluate the mutation frequencies in different sub-groups of ICI scores and somatic cells, with correlation coefficients calculated using Spearman's analysis.

3. Results

3.1 Altered gene expression due to cuproptosis gene variants in STAD

This study identified 19 genes and analyzed their expression in healthy and malignant tissues using the TCGA-STAD dataset. Figure 1A shows the upregulation and downregulation of some genes. Summarizing the prevalence of copy number variations (CNVs) and cellular mutations in CRGs within STAD. Genetic heterogeneity was observed in just 99 out of 431 samples (22.97%). NLRP3 and ATP7B have mutation frequencies of 4% and 3%, respectively (Figure 1B). Figure 1C illustrates the genomic locations of CNVs in the CRGs. There was a generalized change in the CNV of 19 genes. In addition, the CRGs interaction network diagrams were utilized to illustrate their interactions (Figure 1D). According to further studies on the frequency of CNV substitutions, the frequency of CNV amplification was greater in NLRP3 and LIPT2, and conversely CNV deletions were more prevalent in genes including FDX1, DBT, and CDKN2AFigure 1E). Research indicates that CRGs exhibit differential expression patterns in STAD, implying their crucial involvement in STAD development and progression.

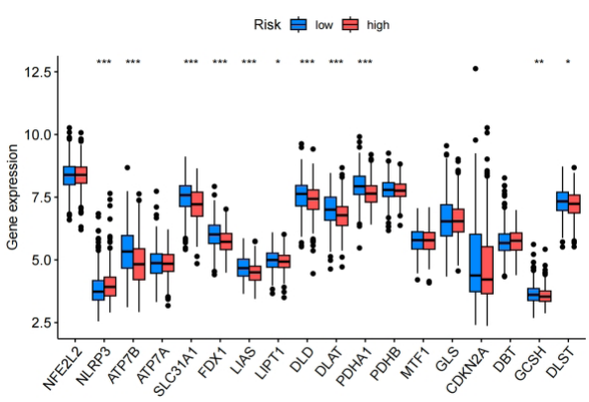

A

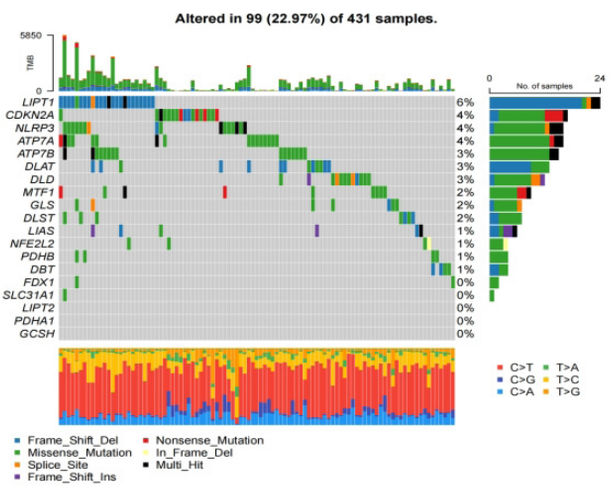

B

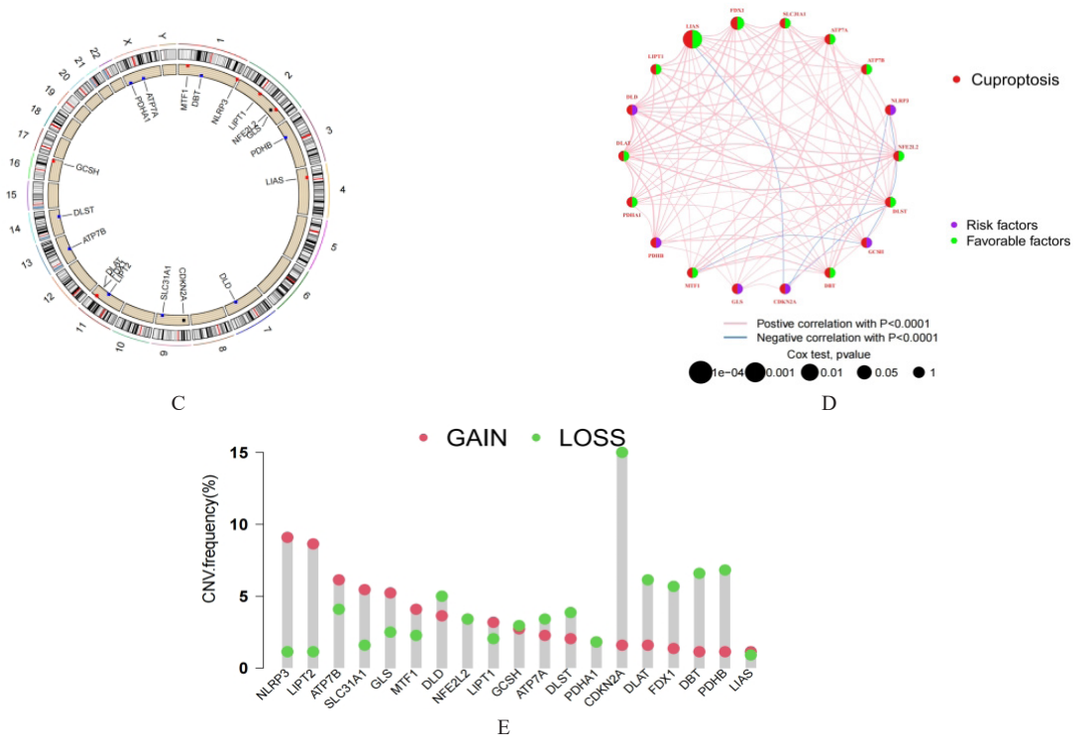

Figure 1. (A) differential expression of CRG; (B) CRG somatic mutation rate in STAD patients; (C) The chromosome distribution of CNV in CAG; (D) CAG is part of the PPI network; (E) The frequency of CNV changes is indicated by green dots indicating downregulation and red dots indicating upregulation, with P<0.05 indicating statistical significance.

3.2 Gene enrichment analysis pertaining to cuproptosis

The correlation between CRG expression levels and patient prognosis was studied, and it was found that the expression levels of 13 genes were strongly correlated with prognosis, among which the expression of 9 genes such as ATP7A was positively correlated with good prognosis. According to KEGG and GO enrichment studies, the growth of the digestive tract and xenobiotic stimulation are the main causes of gene enrichment. (Figure 2A and 2B).

3.3 Utilizing cuproptosis genes for tumor categorization and immune infiltration analysis

Using the GSE84433 dataset, unsupervised clustering was performed on the expression of 19 CRGs in STAD samples, and the differentiation was most pronounced at k=2 (Figure 2A). The PCA scatter plot also showed significant differences between the two subtypes, with k=2 being the most suitable (Figure 2B). The expression of CRG among subtypes showed significant differences (P<0.05) in 13 genes including LIAS (Figure 2F). A notable disparity in tumor stage was evident between the two groups. The biological activity of CRGs was investigated using GSVA analysis, wherein the onco-genic activation mechanisms included (Figure 2E). Survival analysis demonstrated significantly improved survival outcomes for group B compared to group A(Figure 2G).

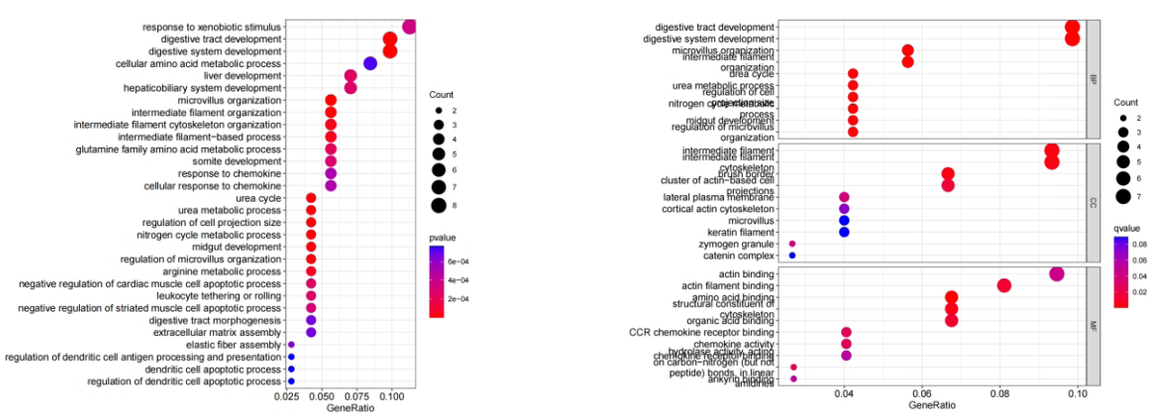

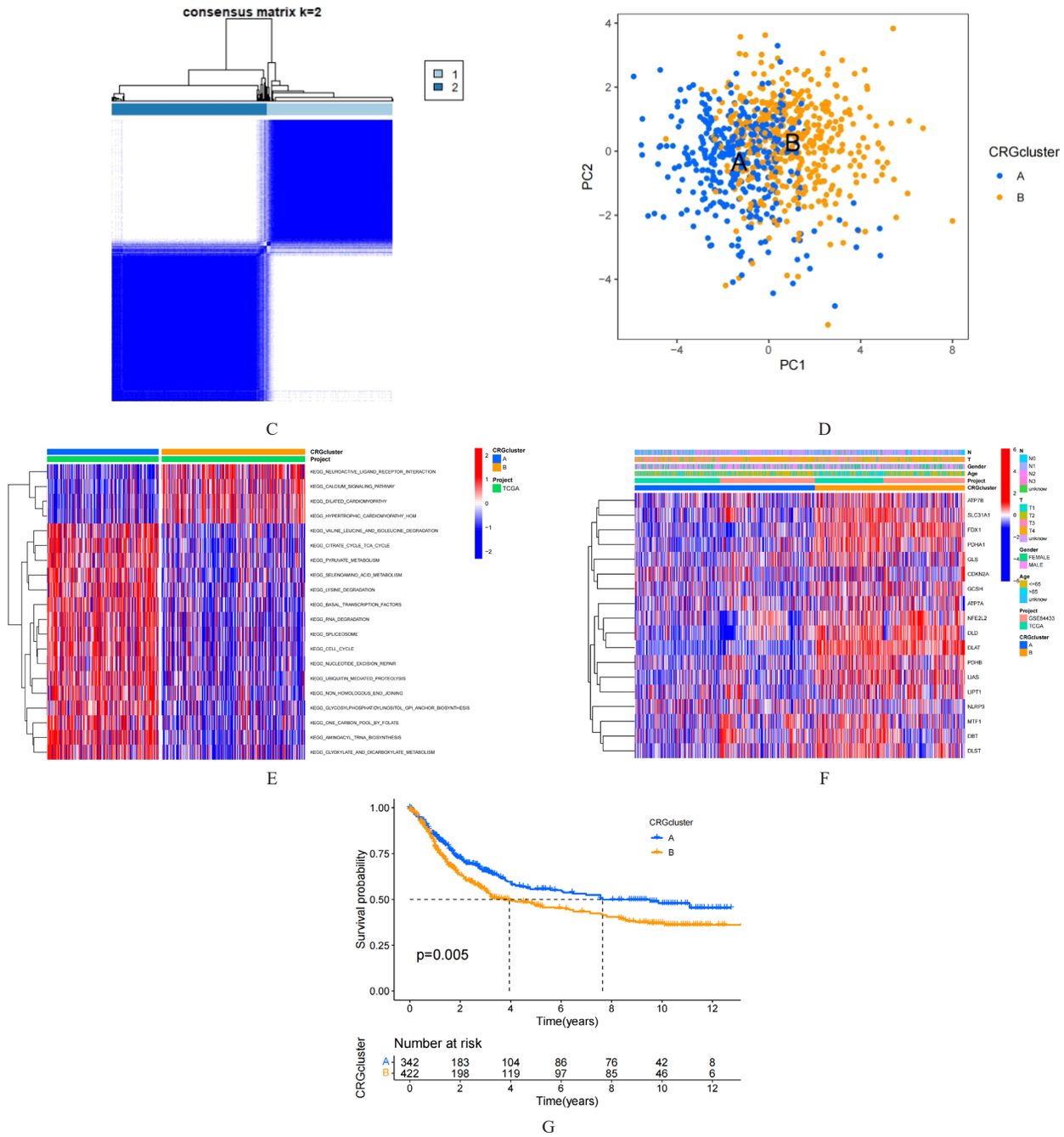

Figure 2. (A) KEGG enrichment; (B) To enrich the analysis; (C) Coherent clustering screening of molecular subgroups; (D) Different subtypes of PCA; (E) GSVA study, red and blue indicate positive and negative correlation pathways; (F) Differential expression analysis of CRGs; (G) Survival analysis of subtypes A and B using logarithmic rank test and KM plot.

3.4 Developing and assessing risk prediction models based on CRG scores

The predictive genes for STAD were identified by the LASSO regression method, considering the unique characteristics of each STAD patients. Two models were built with the identified genes: a prognostic model and a minimal regression model. These models assigned a CRG score to individual patients, creating a quantitative CRG scoring system (Figure 3A). K-W analysis was established to confirm the correlation between CRG scores and CRG groupings. The analysis revealed that group B was associated with higher scores and group A with lower scores (Figure 3B and 3C). Elevated CRG scores correlated with worse prognosis for patients in both groups. K-M analysis showed that the survival rate of the high-risk group was lower than that of the low-risk group (Figure 3D). The alluvial plot displays patient characteristics, with low CRG scores indicating good survival and high scores indicating poor survival (Figure 3E). Copper poisoning is associated with gene expression in patients with different risks (Figure 3F).

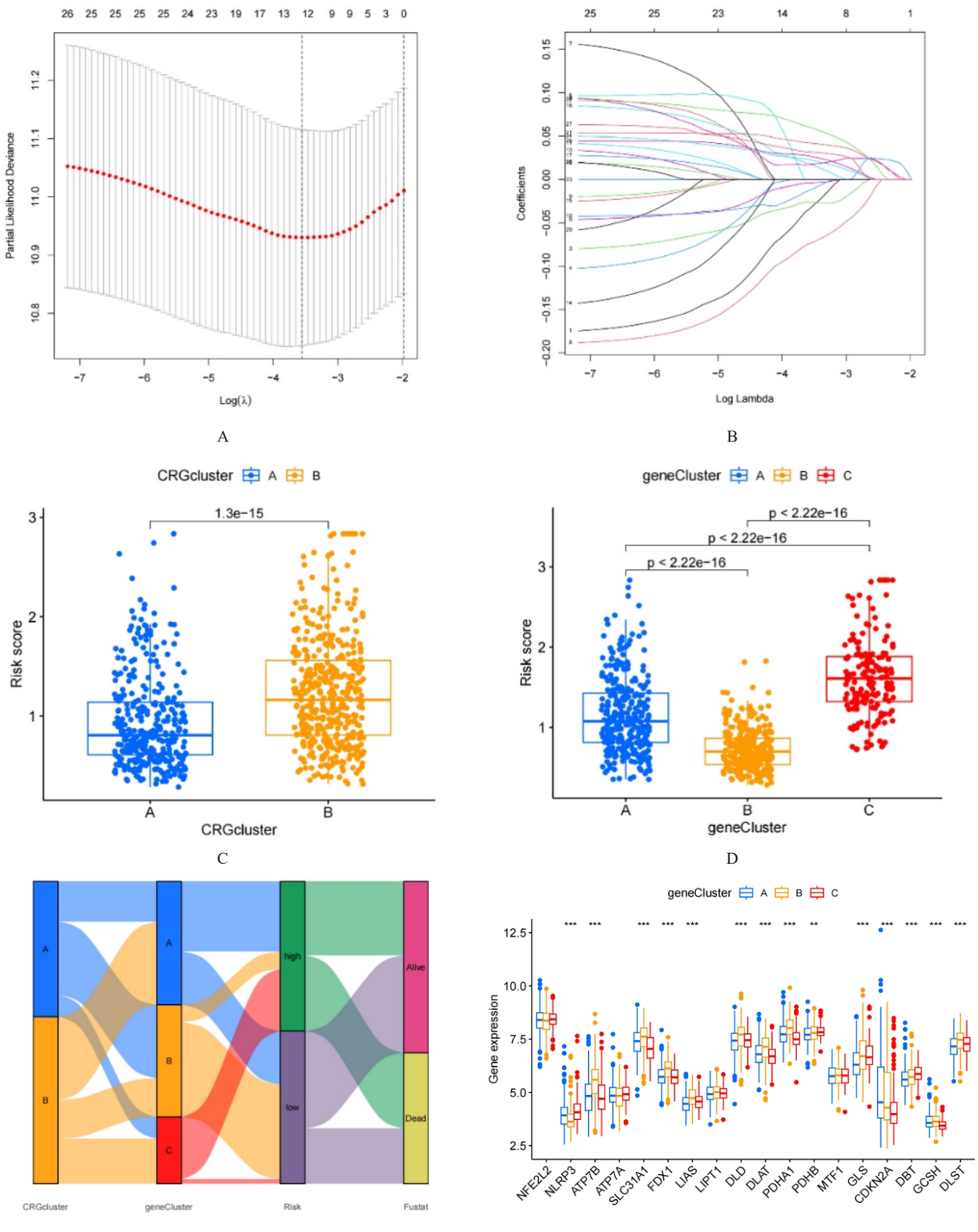

Figure 3. (A) Plotting partial likelihood bias on log(Lambda). (B) LASSO regression analysis.(C) Risk ratings for molecular subtypes A and B were analyzed differently. (D) Differential analysis of risk scores for three genotypes, A, B, and C. (E) Alluvial plots of the process of constructing prognostic models with different molecular subcategories, genotypes, and risk scores.(F) Distinct examination of CRG expression.

3.5 Evaluating the predictive power of the risk models

According to the median threshold and risk score, patients were divided into high-risk or low-risk groups, with the high-risk group having a poorer prognosis (Figure 4A). ROC curve analysis shows the predictive performance for 1, 3, and 5 years, with AUC values shown in Figure 4B. The risk score of the experimental queue is positively correlated with survival outcomes, with higher risk scores leading to higher mortality rates (Figure 4C). The Train cohort results, displayed in Figure 4D, were consistent with the Test cohort findings, where higher risk scores corresponded to reduced survival, supporting the validity of the model.

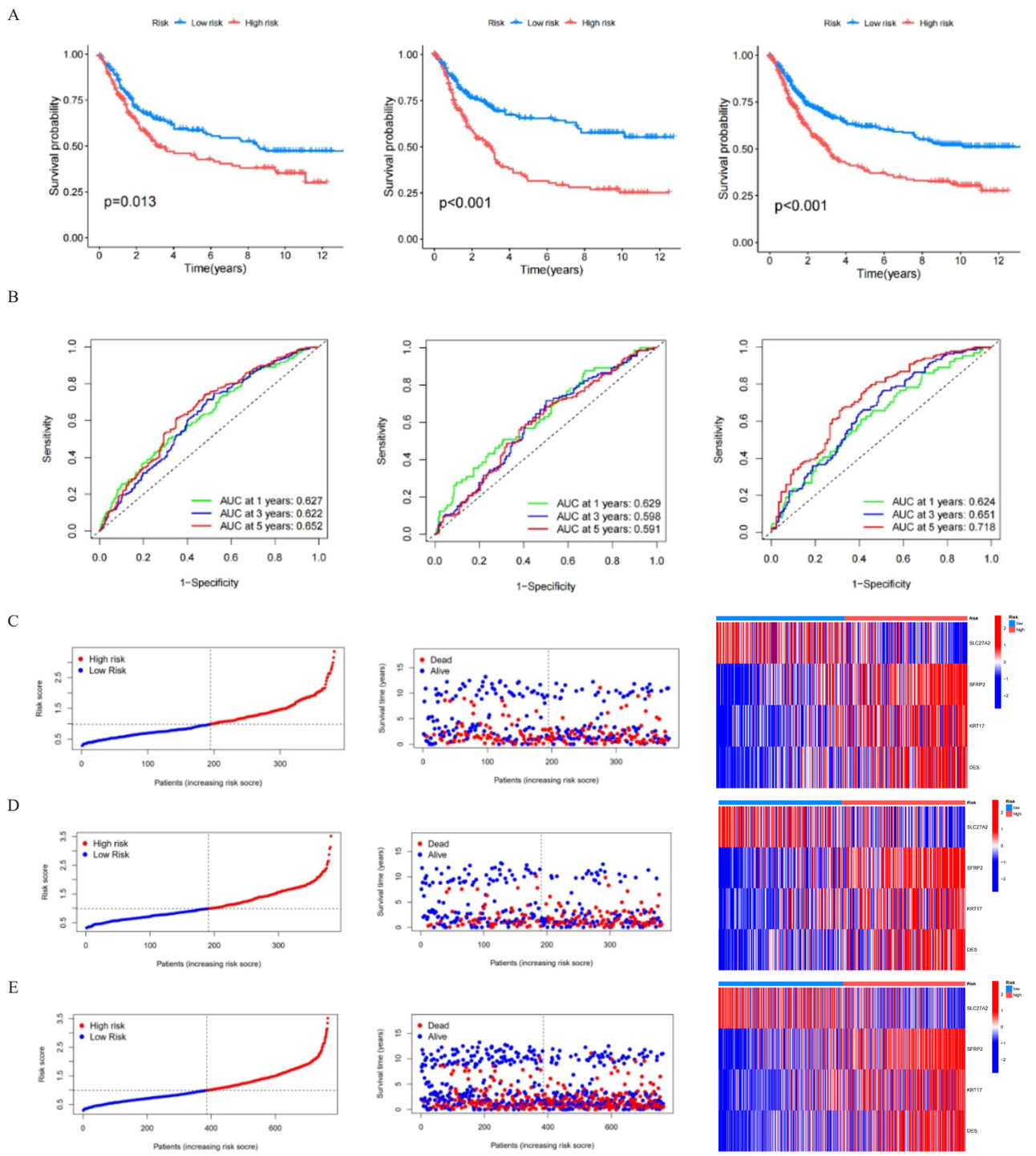

Figure 4. (A) Survival analysis of Test and Train groups. (B) Sensitivity and specificity of ROC curves for predicting survival at 1, 3, and 5 years. (C) Risk scores, survival status, and heatmap of Test group. (D) Risk scores, Train group heatmap, and survival status. (E) Full sample heatmap, risk scores, and survival status.

3.6 Comparison of immunoreactivity between subgroups

According to STAD immune infiltration analysis, there were more innate immune cells in the tumor microenvironment of group B (Figure 5A). Figures 5B-G show that high CRG risk scores are associated with high concentrations of various immune cell types. Risk score is positively correlated with immune and matrix scores (Figure 5H). The association analysis between immune cell populations and four key genes shows that there is a significant correlation between most immune cells, such as SLC27A2, which is negatively correlated with memory B cells and regulatory T cells, and positively correlated with M0 macrophages; SFRP2 is negatively correlated with CD4 memory cells in activated T cells (Figure 5I).

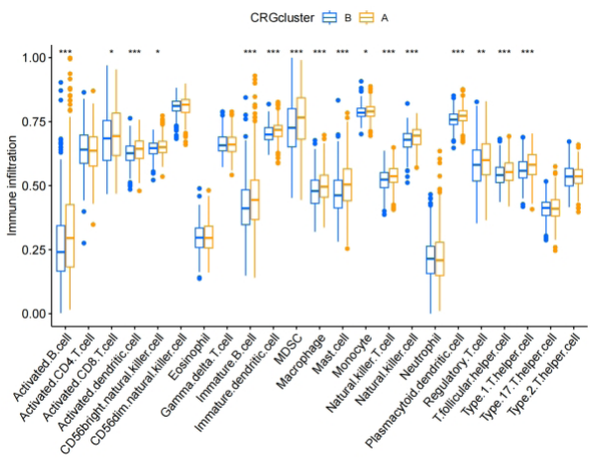

A

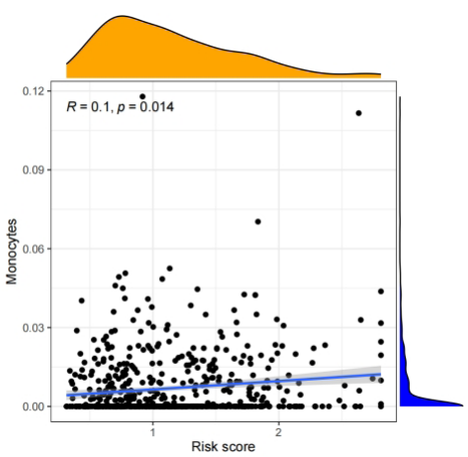

B

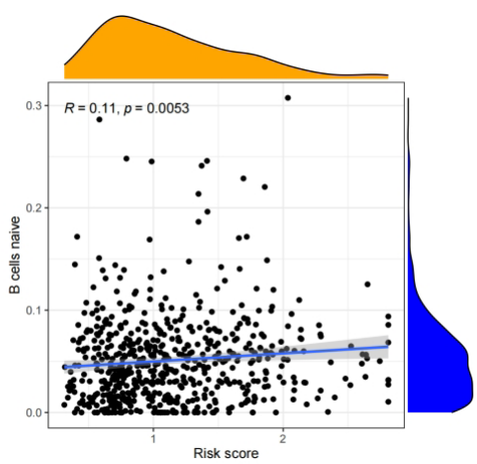

C

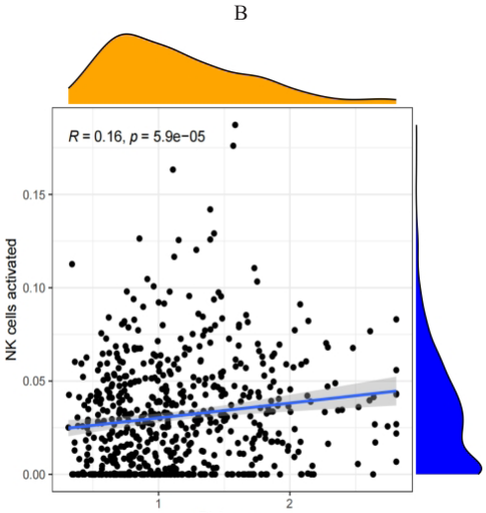

D

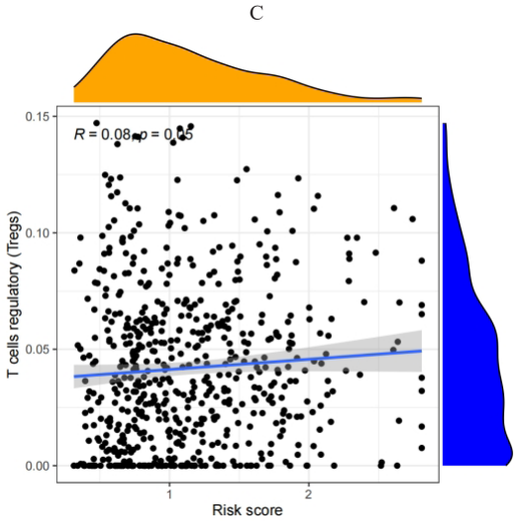

E

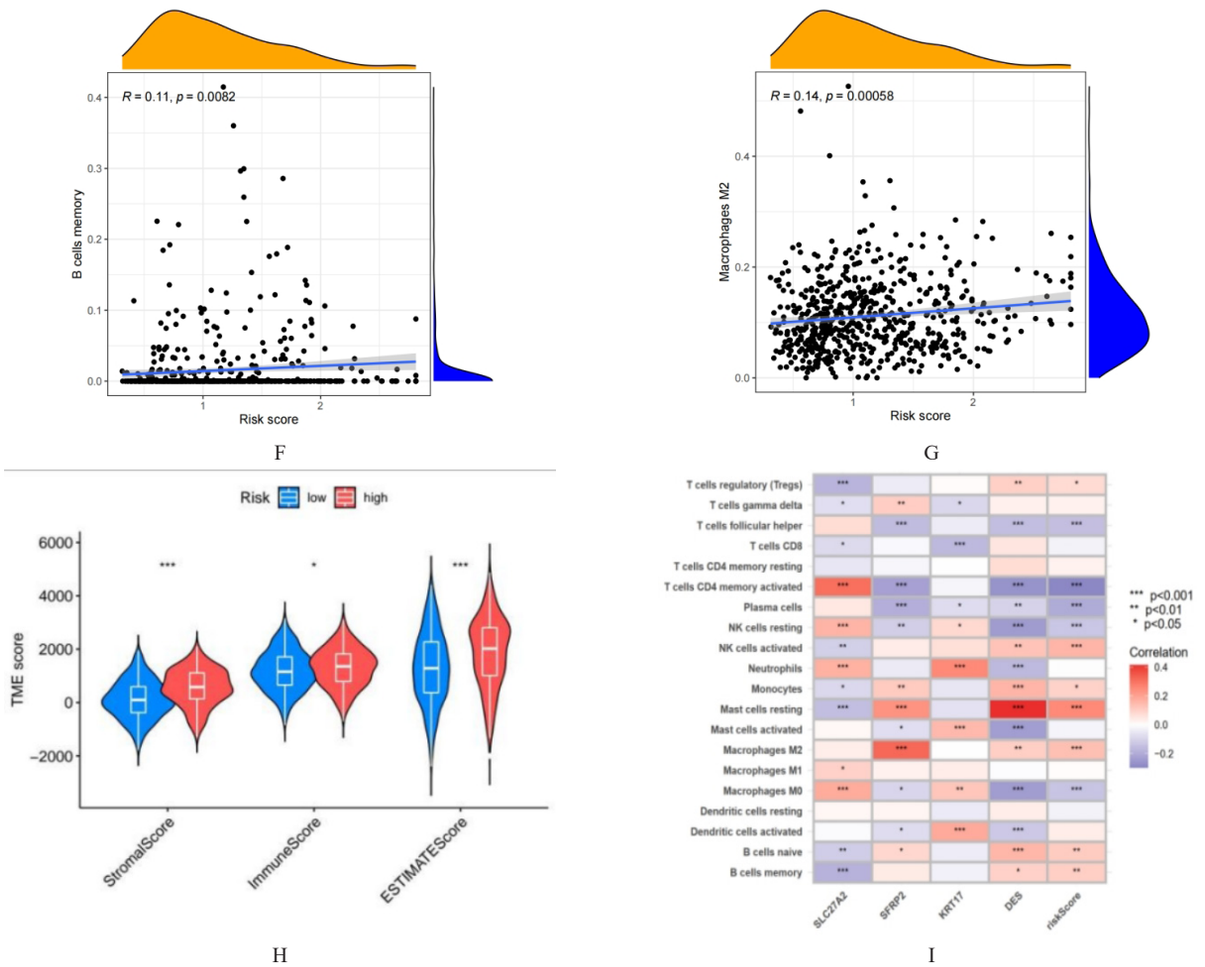

Figure 5. (A) Two clusters where TME-infiltrating cells are common.(B-G) Correlation analysis between immune cell risk scores. (H) Analysis of variance between CRG risk score and immune/blood gas/estimate score. (I) Correlation between key genes and large number of immune cells. p < 0.05 was considered statistically significant. denotes P < 0.05, ** denotes P < 0.01, * denotes P < 0.001.**

3.7 Construction and evaluation of column charts based on CRG scores

Based on the comprehensive patient characteristics (gender, age, TNM stage) and CRG risk score, a column chart was drawn to predict the overall survival rate at 1, 3, and 5 years (Figure 6A). An increase in score indicates poorer clinical outcomes. The calibration curve evaluates the predictive ability of the column chart and shows that the model predicts accurately (Figure 6B).

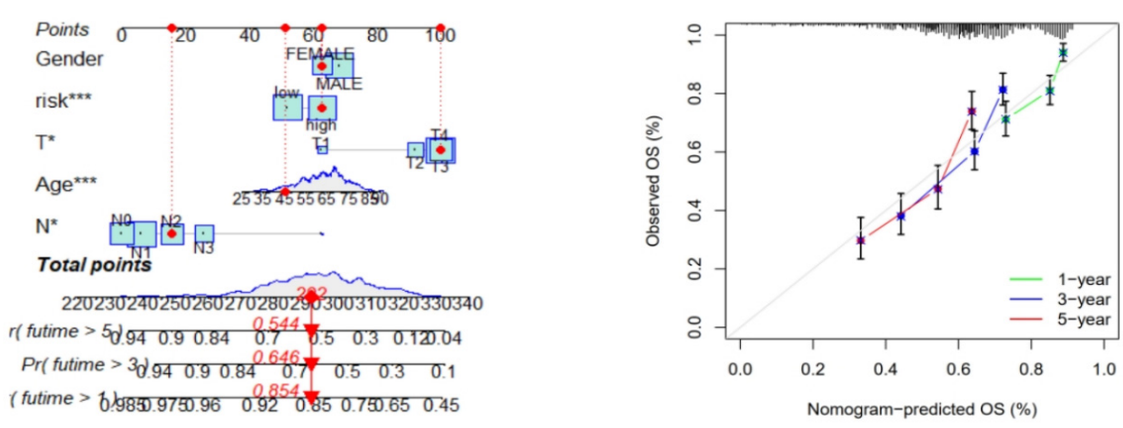

Figure 6. (A) Nomogram predicting OS at 1, 3, and 5 years in patients with STAD.(B) nomogram correction curve.

3.8 Analysis of the relationship between the TMB and MSI and the CRG score

To get further insight into the immunological traits of various risk subtypes, we looked at differences in the distribution of somatic substitutions among various CRG_score groups (Fig 7A and 7B).Twenty genes were found to have the greatest frequencies of mutation in the two risk categories. Based on these findings, it appears that missense mutations predominated among the two types of mutations. In both groups, the mutation rates for TTN, TP53, and MUC16 were greater than 20%. This suggests that they were common in both groups. The likelihood of mutation is higher in the low-risk group than in the high-risk group. There is a negative correlation between TMB and CRG scores (Figure 7C). The high-risk group had fewer MSI-H patients (10% vs 25%) (Figure 7D), and the MSI-H group had the lowest CRG score (Figure 7E).

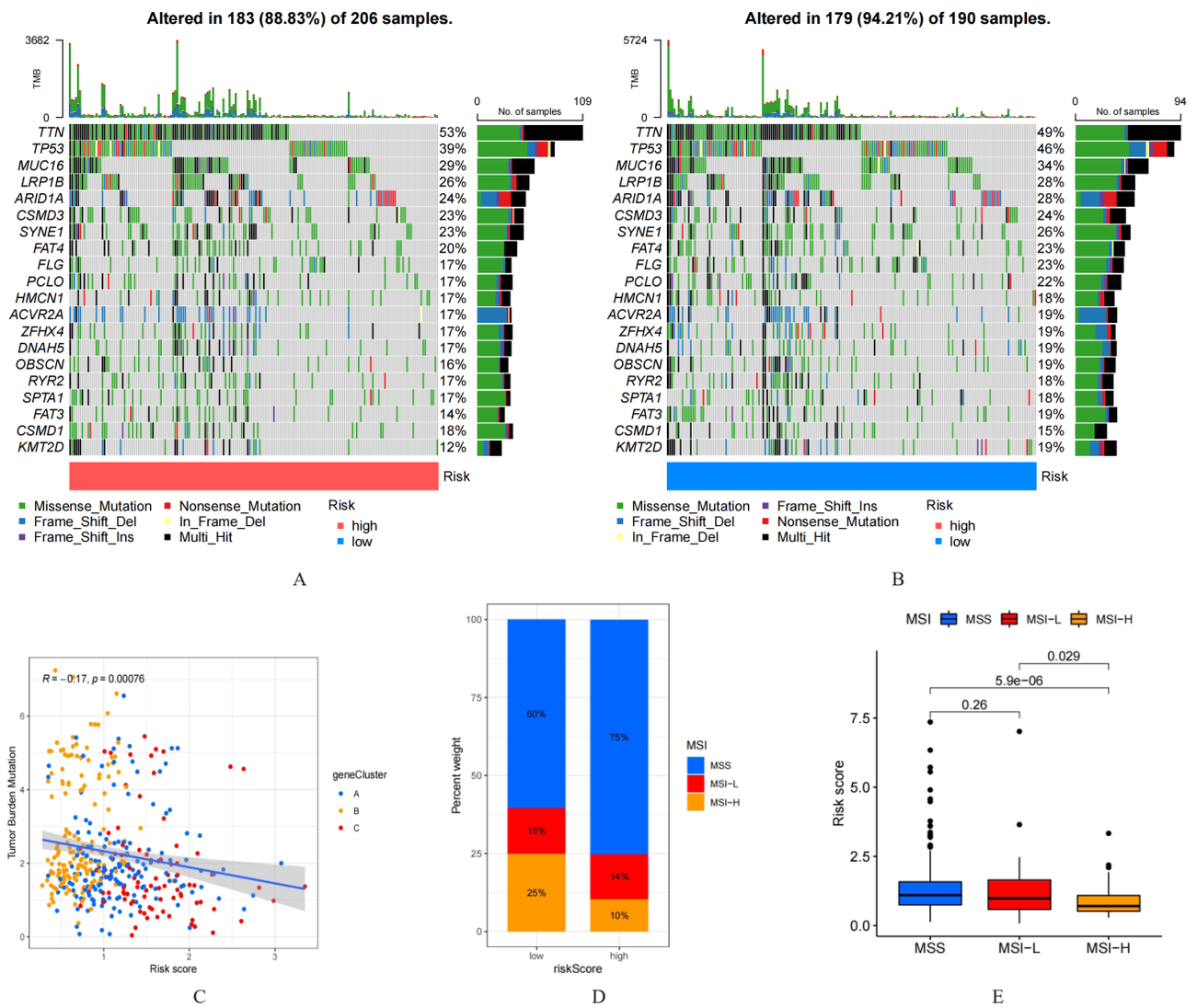

Figure 7. CRG_score correlation analysis using TMB and MSI. (A, B) Using the high and low CRG scores, a graph representing the genomic alterations brought about by somatic mutations has been created. (C)Correlation between TMB and CRG scores (D) The variance in the percentage of distinct microsatellite instability statuses between the two vulnerable subgroups. (E) Variation in CRG_score among distinct status groups for microsatellite instability

3.9 Drug sensitivity analysis

To evaluate the sensitivity of LR and HR groups, anti-cancer drug analysis was selected. Patients with elevated CRG values have decreased IC50 values for Elesclomol, dasatinib, and bleomycin. In contrast, patients with lower CRG values exhibited significantly decreased IC50 values for the chemotherapy agents Gemcitabine, Bosutinib, and Metformin, implying that CRG values are associated with drug sensitivity in STAD patients (Figure 8A-F).

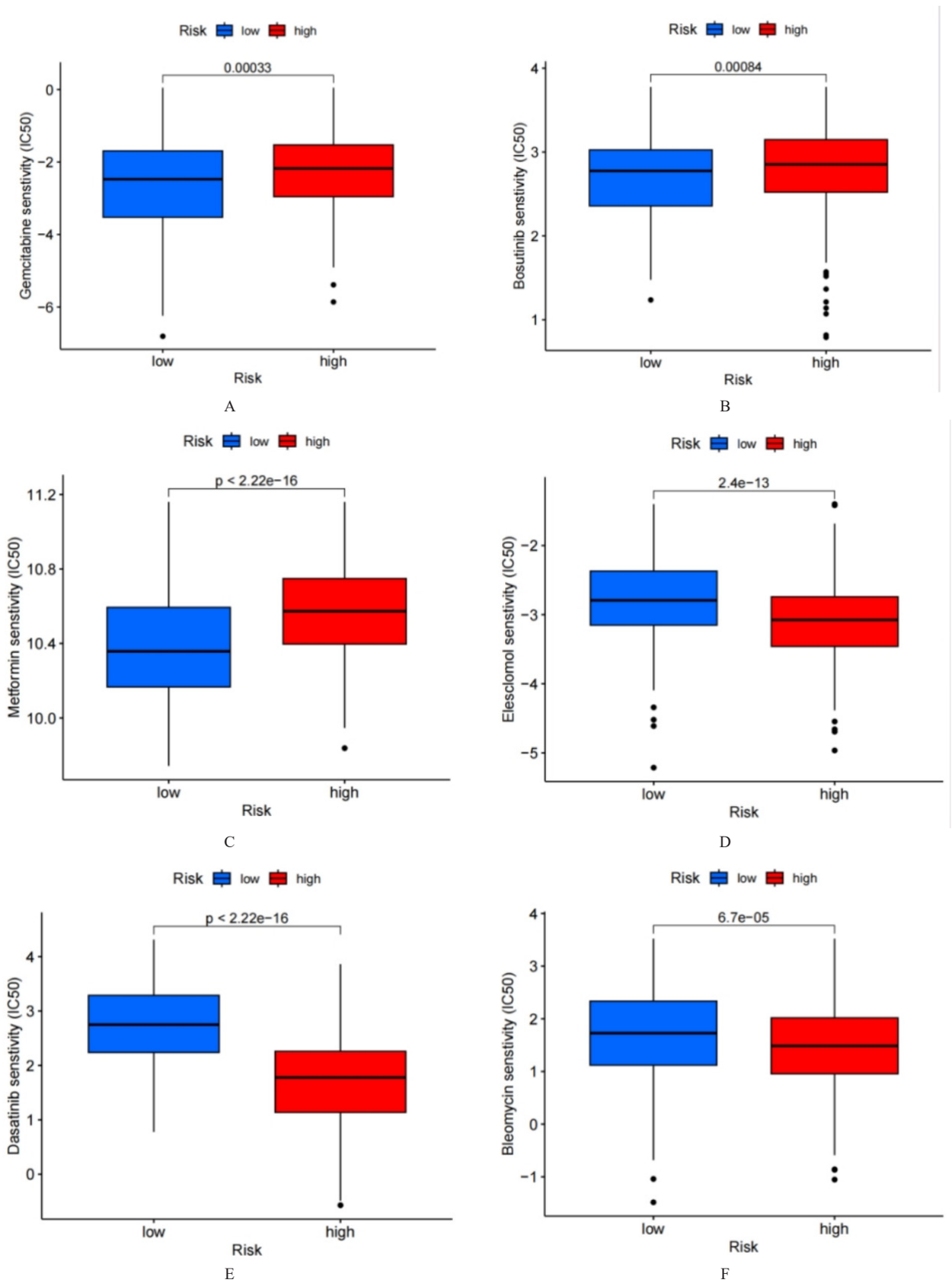

Figure 8. Predicted half-maximal inhibitory concentration (IC50) values. (A-F) IC50 values for six chemotherapeutic agents.

4. Discussion

STAD ranks among the top three most prevalent and deadly malignancies in China, placing a significant burden on the healthcare system. Its development is influenced by multiple factors, such as lifestyle, heredity, and environmental conditions. Timely screening and endoscopic detection are often lacking, resulting in a low early diagnosis rate (<10%) for STAD in China. About half of the patients present with metastatic tumors, predominantly peritoneal metastasis (61%-80%), at the time of initial diagnosis [30]. The current treatment of STAD mainly includes endoscopic and surgical local resection, chemotherapy, radiotherapy, biotargeted therapy, and immunotherapy, etc. [31].

Analyzing transcriptomic data from extensive public repositories like TCGA and GEO enables a thorough comprehension of the genetic terrain, discovery of novel biomarkers, evaluation of treatment options, and prognostic predictions [32,33].

Dysregulation of copper homeostasis is implicated in numerous pathologies. Research indicates that copper plays a crucial role in cellular proliferation, blood vessel formation, and cancer progression [34]. However, when concentrations are higher than what is necessary to maintain cellular equilibrium, it can be harmful to cells. Excessive copper induces mitochondrial mediated cell death by interacting with components of the lipidated TCA cycle[35], and the mechanism is still unclear (leading to accumulation of lipidated proteins, depletion of iron sulfur cluster proteins, protein toxicity stress, and ultimately cell death).Clusters B and C displayed the poorest overall survival and elevated CRG scores across the three gene clusters. Consistently, higher CRG scores correlated with worse clinical outcomes, implying their prognostic value.

Immune and stromal cells are key components of TME, closely related to the clinical characteristics and patient prognosis of STAD. The ESTIMATE algorithm predicts TME and shows a significant increase in immune and stromal scores in the high CRG score group. This implies a correlation between cuproptosis and TME, advancing STAD development and progression. Previous research indicates that dysregulated immune cells facilitate STAD advancement and regulate cell death, while immunotherapy targeting checkpoints improves survival in advanced cancer patients [36]. Utilizing CRG assessment, a precise prognostic framework was developed to forecast alterations in the tumor microenvironment. Thoroughly examining CRG and clinical factors can help evaluate the efficacy of immunotherapy[37]. There are significant differences in clinical prognosis, genetic changes, and immune cell infiltration among the patient groups. Integrate age, tumor staging, and CRG score to create a composite graph of enhanced predictive framework.

Copper mutation is a novel form of cell death that relies on the interaction between copper ions and tricarboxylic acid cycling components, reducing mitochondrial respiratory reserve capacity [38]. In addition, intermediates accumulated by TCA cycle can contribute to cancer progress. Considering these findings, we proposed that excessive copper disrupting the TCA cycle and the resulting mitochondrial respiration could potentially hinder STAD cell proliferation, thus impeding tumor progression. Genes linked to cell death caused by copper could serve as therapeutic targets for STAD, while copper-associated genes may offer novel predictive markers for STAD treatment outcomes and prognosis. This provides fresh insights into the function of copper ions in STAD by modulating specific signaling cascades and influencing metabolic pathways.

The low CRG score group showed significantly higher IC50 values for 9 molecules, while the high CRG score group was more sensitive to these treatments. Evaluated the responsiveness of the CRG scoring queue to commonly used anti-cancer drugs to guide treatment decisions. The CRG score can be used to evaluate patient CRG expression and tumor microenvironment characteristics.This approach aids in determining the tumor's immunophenotype and offers insights for more precise and potent treatment plans. Moreover, CRG score was used as a standalone prognostic indicator to forecast immunotherapy effectiveness in STAD patients. With our findings, we may be able to pinpoint many STAD immunophenotypes, develop targeted and accurate immunotherapy, and boost the therapeutic effectiveness of immunotherapy for patients.

5. Conclusion

Using a variety of in silico techniques, we examined the possible function of CRGs in the TME of STAD tissues by analyzing specific cohorts from GEO and TCGA. There were differences between the two groups of clinical and immunological characteristics. Consequently, a predictive nomogram and a signature connected to CRG were created. Low CRG score is associated with high microsatellite instability, immune activation, high tumor mutation burden, improved survival rate, and higher immune responsiveness to ICI. CRG may affect the tumor immune microenvironment and clinical outcomes of STAD patients, which is of great significance for evaluating immune therapy and targeted therapy response, and can predict treatment response and prognosis of STAD patients.

Acknowledgments

Author Contributions: Conceptualization, J.Y.L.; methodology, H.X.R, D.C.Z.; formal analysis, H.H G,W.H.L.;

investigation, S.J.X.; data curation, X.Y.W.; writing—original draft preparation, Y.C.L.; visualization, R.B.P.

Funding: This research received no external funding.

Data Availability Statement: We utilized public dataset GSE84433, which was generously contributed by Cheong J, Jang E, Kim H, Park J, Kim J, Kim H, Shin Y, Son H, Choi Y, Hyung W, Noh S, Suh J, Huh Y.We extend our gratitude to the respective research teams for their efforts in creating and maintaining these resources.

Conflicts of Interest: The authors declare no conflicts of interest.

Abbreviations

Stomach adenocarcinoma (STAD); Kaplan-Meier analysis(K-M analysis); Kruskal-Wallis test(K-W test); Cuproptosis-related genes(CRGs); Different-expressed genes(DEGs); Small Cell Lung Cancer(SCLC);immune checkpoint inhibitor(ICI);microsatellite instability(MSI);tricarboxylic acid cycle(TCA cycle);Tumor Mutation Burden(TMB)

References

[1] Goga A B, Naroua H, Kadri C.A Hybrid Learning Algorithm for Breast Cancer Diagnosis[J].Journal of Intelligent Learning Systems and Applications, 2024, 16(3):262-273.DOI:10.4236/jilsa.2024.163014.

[2] Kim G H, Lee Y C, Kim T J,et al.Trends in colorectal cancer incidence according to an increase in the number of colonoscopy cases in Korea[J].World Journal of Gastrointestinal Oncology, 2024, 16(1):51-60.DOI:10.4251/wjgo.v16.i1.51.

[3] AHMAD ALHASKAWI, SOHAIB HASAN ABDULLAH EZZI, YANZHAO DONG, et al. Recent advancements in the diagnosis and treatment of acral melanoma[J]. Journal of Zhejiang University SCIENCE B,2024,25(2):106-122. DOI:10.1631/jzus.B2300221.

[4] FATMA KHALLAF, WALID EL-SHAFAI, EL-SAYED M. EL-RABAIE, et al. A novel hybrid cryptosystem based on DQFrFT watermarking and 3D-CLM encryption for healthcare services[J]. Frontiers of Information Technology & Electronic Engineering,2023,24(7):1045-1061. DOI:10.1631/FITEE.2200372.

[5] Dashtaki M, Moradi Z, Ghasemi F S.Estimating the Survival Rate in Glioblastoma Multiforme Patients who Received a Peptide Vaccine: A Systematic Review and Meta-analysis[J].Current drug targets-The International journal for timely in-depth reviews on drug targets, 2023, 24(12):998-1007.

[6] Barkhoudarian G, Zhou D, Avery M B,et al.Comparative Analysis of Endoscope Obscuration With Utilization of an Endonasal Access Guide for Endonasal Skull Base Surgery[J].Operative Neurosurgery, 2024, 28(2):203-209.DOI:10.1227/ons.0000000000001267.

[7] SHUNUO SHANG, YINGQIAN SHI, YAJIE ZHANG, et al. Artificial intelligence for brain disease diagnosis using electroencephalogram signals[J]. Journal of Zhejiang University SCIENCE B,2024,25(10):914-940. DOI:10.1631/jzus.B2400103.

[8] Parente A, Lurje I, Schlegel A.Mapping new mechanisms: Hypothermic oxygenated perfusion attenuates the immune response after human liver transplantation[J].Liver Transplantation, 2024, 31(3):262-264.DOI:10.1097/LVT.0000000000000534.

[9] SHENG ZENG, SHAOQIANG XING, YIFEI ZHANG, et al. Nano-Bacillus Calmette-Guérin immunotherapies for improved bladder cancer treatment[J]. Journal of Zhejiang University SCIENCE B,2024,25(7):557-567. DOI:10.1631/jzus.B2300392.

[10] KUN ZHANG, QIQUAN YU, QI BAO, et al. Efficacy observation of acupuncture plus point application for pain after thoracoscopic radical lung cancer surgery[J]. Journal of Acupuncture and Tuina Science,2023,21(6):455-459. DOI:10.1007/s11726-023-1404-2.

[11] WEN XIE, WEIDONG LIU, LEI WANG, et al. Roles of THEM4 in the Akt pathway: a double-edged sword[J]. Journal of Zhejiang University SCIENCE B,2024,25(7):541-556.DOI:10.1631/jzus.B2300457.

[12] CHUNYU SONG, XUE GUAN, CHANGMING XIE, et al. Inhibiting PI3K/AKT/mTOR signaling by metal-organic frameworks for overcoming multiple drug resistance in chemoradiotherapy[J]. Science China Materials,2024,67(5):1631-1645.DOI:10.1007/s40843-023-2774-8.

[13] Gashi Z, Hamza A, Ukimeri B,et al.A Rare Case of Gastric Metastasis from a Rare Case of Mucosal Malignant Melanoma[J].Open Access Macedonian Journal of Medical Sciences, 2024, 12(2):362-364.DOI:10.3889/oamjms.2024.11917.

[14] Xiao D, Chen T, Zhang T,et al.Transdermal treatment for malignant melanoma by aptamer-modified tetrahedral framework nucleic acid delivery of vemurafenib[J].Chinese Chemical Letters, 2024, 35(4):260-267.DOI:10.1016/j.cclet.2023.108602.

[15] Boby A, Dugan M M, Ghali H,et al.Isolated Limb Infusion as First, Second, or Third or Later-Line Therapy for Meta-

static In-Transit Melanoma:[J].Cancer Control, 2024, 31(2):475-481.DOI:10.1177/10732748241297326.
[16] Song R, Yin S, Wu J,et al.Neuronal regulated cell death in aging-related neurodegenerative diseases:key pathways and therapeutic potentials[J].Neural Regeneration Research, 2025, 20(8):2245-2263.DOI:10.4103/NRR.NRR-D-24-00025.
[17] Lim S M, Schalm S S, Lee E J,et al.BLU-945, a potent and selective next-generation EGFR TKI, has antitumor activity in models of osimertinib-resistant non-small-cell lung cancer:[J].Therapeutic Advances in Medical Oncology, 2024, 16(3):209-249.DOI:10.1177/17588359241280689.
[18] Kerur B, Fiedler K, Stahl M,et al.Utilization of Antitumor Necrosis Factor Biologics in Very Early Onset Inflammatory Bowel Disease: A Multicenter Retrospective Cohort Study From North America[J].Journal of pediatric gastroenterology and nutrition, 2022, 75(1):64-69.DOI:10.1097/MPG.0000000000003464.
[19] Guha A, Panda S, Chakraborty P,et al.Malignant Mixed Germ Cell Tumor of the Ovary[J].Research and Reviews in Pediatrics, 2024, 25(1):19-21.DOI:10.4103/rrp.rrp_15_23.
[20] Tokui H, Yahata H,Yasuhiro OkabeNaomi MagarifuchiShoji MaenoharaKazuhisa HachisugaHiroshi TomonobeKeisuke KodamaHiroshi YagiMasafumi YasunagaIchiro OnoyamaKazuo AsanomaYoshinao OdaMasafumi NakamuraKiyoko Kato.Complete reduction surgery of a huge recurrent adult granulosa cell tumor after neoadjuvant chemotherapy-[J].International Cancer Conference Journal, 2024, 13(2):162-166.DOI:10.1007/s13691-024-00659-5.
[21] Cheng N H, Smith D, Errickson C A S.A rare case of cutaneous granular cell tumor with unusual Melan-A expression in a child[J].Journal of cutaneous pathology, 2024, 51(6):434-438.DOI:10.1111/cup.14619.
[22] Sahu P K, Malla S, Khuntia M R S N M.SMART CROP PREDICTICTION USING STATISTICAL TECHNIQUES OF MACHINE LEARNING THROUGH IoT[J].journal of theoretical and applied information technology, 2024, 102(7):3131-3142.
[23] More K S, Wolkersdorfer C.Exploring Advanced Statistical Data Analysis Techniques for Interpolating Missing Observations and Detecting Anomalies in Mining Influenced Water Data[J].ACS ES&T Water, 2024, 4(3):1036-1045. DOI:10.1021/acsestwater.3c00163.
[24] Chen Z, Zhang L,Yao LvShenyang QuWenjun LiuKai WangSong GaoFeng ZhuBili CaoKun Xu.A genome assembly of ginger (Zingiber officinale Roscoe) provides insights into genome evolution and 6-gingerol biosynthesis[J].The Plant Journal, 2024, 118(3):682-695.DOI:10.1111/tpj.16625.
[25] Zhao X, Liu J, Fu X,et al.Whole-genome characterization of CKX genes in Prunus persica and their role in bud dormancy and regrowth[J].Journal of Integrative Agriculture, 2024, 23(12):4058-4073.DOI:10.1016/j.jia.2024.09.002.
[26] Wang N, Zeng T.Analysis of the expression characteristics and clinical value of immune function indicators in patients with human immunodeficiency virus infection[J].Pakistan journal of medical sciences. 2024, 40(10):2233-2237.
[27] Wang P C, Zhao Q Y, Zhu X F,et al.OZONE THERAPY AMELIORATES LPS-INDUCED ACUTE LUNG INJURY IN MICE BY INHIBITING THE NLRP3/ASC/CASPASE-1 AXIS[J].Shock, 2024, 63(3):487-494.DOI:10.1097/SHK.0000000000002525.
[28] M. REDDY, K. PALMER, D. L. ROLNIK, et al. Role of placental, fetal and maternal cardiovascular markers in predicting adverse outcome in women with suspected or confirmed pre-eclampsia[J]. Ultrasound in Obstetrics & Gynecology,2022,59(5):596-605. DOI:10.1002/uog.24851.
[29] Barbosa I G, Lima A D O, Edwards J R,et al.Development of track component health indices using image-based railway track inspection data:[J].Proceedings of the Institution of Mechanical Engineers, Part F: Journal of Rail and Rapid Transit, 2024, 238(6):706-716.DOI:10.1177/09544097231224825.
[30] Intralawan T, Methasate A, Parakonthun T,et al.Conversion Therapy for Gastric Cancer with Peritoneal Metastasis[J]. Siriraj Medical Journal, 2024, 76(8).DOI:10.33192/smj.v76i8.268224.
[31] Seebauer C T, Wiens B,Hintschich, Constantin A.Platz Batista da Silva, NataschaEvert, KatjaHaubner, FrankKapp, Friedrich G.Wendl, ChristinaRenner, KathrinBohr, ChristopherKuehnel, ThomasVielsmeier, Veronika.Targeting the microenvironment in the treatment of arteriovenous malformations[J].Angiogenesis, 2024, 27(1):91-103.DOI:10.1007/s10456-023-09896-3.
[32] Kwinten K J J, Lemain V A, De Hullu J A,et al.Cervicovaginal specimen biomarkers for early detection of ovarian and endometrial cancer: A review[J].Cancer Medicine, 2024, 13(14).DOI:10.1002/cam4.70000.
[33] Georgy G S, Laila I M I, Amer M E,et al.Assessment the effect of Dapoxetine and/or Acetaminophen in rats; neurochemicals and oxidative stress biomarkers evaluation[J].Brain Science Advances, 2024, 10(1):56-70.DOI:10.26599/BSA.2023.9050027.
[34] Xu W, Ji J, Diao D,et al.PAI-1 Upregulates YAP1 Expression, Suppresses Retinal Microvascular Endothelial Cell Proliferation, and Promotes Apoptosis Under High Glucose Induction[J]. 2024, 38(1):767-777.DOI:10.23812/j.biol.regul.homeost.agents.20243801.63.
[35] Ardissone A, Ferrera G, Lamantea M E.Phenotyping mitochondrial DNA-related diseases in childhood: A cohort study of 150 patients[J].European journal of neurology: the official journal of the European Federation of Neurological Societies, 2023, 30(7):2079-2091.DOI:10.1111/ene.15814.
[36] Morganti S, Tolaney S M.Role of Immunotherapy in Early- and Late-Stage Triple-Negative Breast Cancer[J].Hematol-

ogy/oncology clinics of North America, 2023, 37(1):133-150.DOI:10.1016/j.hoc.2022.08.014.
[37] Jin J, Mou H, Zhou Y,et al.Nomogram for Predicting Survival Post-Immune Therapy in Cholangiocarcinoma Based on Inflammatory Biomarkers:[J].Cancer Control, 2024, 31(9):557-588.DOI:10.1177/10732748241305237.
[38] Mishra R, Quraishi R, Deep R,et al.An Exploratory Case–Control Study for Mitochondrial DNA G10398A in Bipolar I Disorder Patients with a Family History of Affective Disorders[J].Nigerian Postgraduate Medical Journal, 2024, 31(3):234-239.DOI:10.4103/npmj.npmj_119_24.